microbial biotechnology

Open Access

Experimental validation of *in silico* model-predicted isocitrate dehydrogenase and phosphomannose isomerase from *Dehalococcoides mccartyi*

M. Ahsanul Islam,† Anatoli Tchigvintsev, Veronica Yim, Alexei Savchenko, Alexander F. Yakunin, Radhakrishnan Mahadevan and Elizabeth A. Edwards*

Department of Chemical Engineering and Applied Chemistry, University of Toronto, Toronto, ON M5S 3E5, Canada

Summary

Gene sequences annotated as proteins of unknown or non-specific function and hypothetical proteins account for a large fraction of most genomes. In the strictly anaerobic and organohalide respiring *Dehalococcoides mccartyi*, this lack of annotation plagues almost half the genome. Using a combination of bioinformatics analyses and genome-wide metabolic modelling, new or more specific annotations were proposed for about 80 of these poorly annotated genes in previous investigations of *D. mccartyi* metabolism. Herein, we report the experimental validation of the proposed reannotations for two such genes (KB1_0495 and KB1_0553) from *D. mccartyi* strains in the KB-1 community. KB1_0495 or *Dm*IDH was originally annotated as an NAD^+-dependent isocitrate dehydrogenase, but biochemical assays revealed its activity primarily with $NADP^+$ as a cofactor. KB1_0553, also denoted as *Dm*PMI, was originally annotated as a hypothetical protein/sugar isomerase domain protein. We previously proposed that it was a bifunctional phosphoglucose isomerase/phosphomannose isomerase, but only phosphomannose isomerase activity was identified and confirmed experimentally. Further bioinformatics analyses of these two protein sequences suggest their affiliation to potentially novel enzyme families within their respective larger enzyme super families.

Received 11 November, 2014; revised 12 July, 2015; accepted 7 August, 2015. *For correspondence. E-mail elizabeth.edwards@utoronto.ca; Tel. 416 946 3506; Fax 416 978 8605.
doi:10.1111/1751-7915.12315
†Present address: Department of Chemical Engineering, Massachusetts Institute of Technology, Cambridge, Massachusetts, USA.
Funding Information This research was funded by the University of Toronto, the Natural Sciences and Engineering Research Council of Canada (NSERC), the Government of Canada through Genome Canada and Ontario Genomics Institute (2009-OGI-ABC-1405) and the United States Department of Defense Strategic Environmental Research and Development Program (SERDP). MAI was funded by the Ontario Graduate Scholarship (OGS), the SERDP and Genome Canada funds to EAE and the departmental faculty start-up funds to RM.

Introduction

As one of the smallest free-living organisms, *Dehalococcoides mccartyi* are important for their ability to detoxify ubiquitous and stable groundwater pollutants such as chlorinated ethenes and benzenes into benign or less toxic compounds (Maymó-Gatell *et al.*, 1997; Adrian *et al.*, 2000; 2007a; He *et al.*, 2003; Löffler *et al.*, 2012). Only these strictly anaerobic niche specialists are capable of harnessing energy for growth from the complete detoxification of known human carcinogens, trichloroethene (TCE) and vinyl chloride (VC) (EPA, 2011, Guha *et al.*, 2012) to benign ethene. This energy-conserving metabolic process, termed reductive dechlorination, is catalysed by reductive dehalogenases, the respiratory enzyme system of *D. mccartyi*. Reductive dechlorination, also known as organohalide respiration, is useful not only for the bioremediation of toxic chlorinated solvents, but also a key component to comprehend the recycling of naturally occurring organohalides (Gribble, 2010; 2012). As such, the fundamental understanding of *D. mccartyi* metabolism, including the genes and enzymes involved in metabolic processes, has wide-ranging implications for the remediation of toxic compounds and global element cycling (Gribble, 2012). So far, numerous systems-level studies on *D. mccartyi* metabolism, including the construction of a pan-genome-scale metabolic model (Ahsanul Islam *et al.*, 2010), and various transcriptomic and proteomic analyses (Morris *et al.*, 2006; 2007; Johnson *et al.*, 2008; 2009; Lee *et al.*, 2012), have begun to shed light on key metabolic processes and associated genes.

Although *D. mccartyi* metabolism is well studied, the activities of only a handful of metabolic genes have been experimentally validated. These include an Re-citrate synthase (Marco-Urrea *et al.*, 2011) involved in the tricarboxylic acid (TCA)-cycle, a bifunctional mannosylglycerate (MG) synthase/phosphatase with a potential role in osmotic stress adaptation (Empadinhas *et al.*, 2004), 12 reductive dehalogenases involved in res-

piration and energy conservation (Magnuson *et al*., 1998; 2000; Krajmalnik-Brown *et al*., 2004; Müller *et al*., 2004; Adrian *et al*., 2007b; Tang *et al*., 2013; Wang *et al*., 2014), and two hydrogenases (Jayachandran *et al*., 2004; Nijenhuis and Zinder, 2005) potentially involved in the electron transport chain of *D. mccartyi*. Genome sequences of several strains of these bacteria (Kube *et al*., 2005; Seshadri *et al*., 2005) revealed the presence of ~ 50% hypothetical proteins and proteins with unknown or non-specific functions in their genomes. The primary gene annotations, including the annotations for more than 80 metabolic genes, were reviewed, and in some instances corrected during the construction and manual curation of the genome-wide *D. mccartyi* metabolic model (Ahsanul Islam *et al*., 2010). Also, a recent systems-level study (Ahsanul Islam *et al*., 2014) on *D. mccartyi* transcriptomes provided additional confidence to some of the proposed gene reannotations used in the metabolic model and helped predict putative functions for five hypothetical proteins. One such hypothetical protein was proposed to be a putative bifunctional phosphoglucose isomerase (PGI; EC 5.3.1.8)/ phosphomannose isomerase (PMI; EC 5.3.1.9) from the gene-expression analysis (Ahsanul Islam *et al*., 2014) and metabolic modelling studies on *D. mccartyi* (Ahsanul Islam *et al*., 2010). Another metabolic gene that was primarily annotated as a putative NAD^+-isocitrate dehydrogenase (IDH) (EC 1.1.1.41) was reannotated as a putative $NADP^+$-dependent IDH (EC 1.1.1.42) during the modelling study. However, these proposed reannotations were not supported by any experimental data.

In this study, we report the heterologous expression and biochemical characterization of the aforementioned putative IDH (KB1_0495) and PGI/PMI (KB1_0553) from *D. mccartyi* in KB-1 (Hug, 2012; Ahsanul Islam *et al*., 2014). KB-1 is a mixed enrichment culture containing several strains of *D. mccartyi* (Duhamel and Edwards, 2006; Hug *et al*., 2012). These two genes were selected because they produced soluble proteins when expressed in *Escherichia coli*. The orthologs of these genes in pure strains of *D. mccartyi* (DET0450, cbdbA408, DehaBAV_0427, DhcVS_392, DehalGT_0391, btf_415, dcmb_461, GY50_0375 and DET0509, cbdbA472, DehaBAV1_0485, DhcVS_0450, DehalGT_0448, btf_472, dcmb_518, GY50_0435) are 98–100% similar at the amino acid level (Markowitz *et al*., 2012). Although IDH is an important TCA-cycle enzyme catalysing the formation of 2-oxoglutarate and CO_2 with NAD^+ or $NADP^+$ as a cofactor (Nelson and Cox, 2006; Madigan *et al*., 2010; Kanehisa *et al*., 2011), the physiological role of a bifunctional PGI/PMI in *D. mccartyi* is unclear. PGI, in general, plays a central role in sugar metabolism via glycolysis and gluconeogenesis in all life forms (Hansen *et al*., 2004a,b; Nelson and Cox, 2006), whereas PMI helps to produce precursors for cell wall components, glycoproteins, glycolipids and storage polysaccharides (Hansen *et al*., 2004a; Quevillon *et al*., 2005; Rajesh *et al*., 2012). However, glycolysis is inactive in *D. mccartyi* (Kube *et al*., 2005; Seshadri *et al*., 2005; Ahsanul Islam *et al*., 2010), and cells of these bacteria also lack a typical bacterial cell wall (Löffler *et al*., 2012). The genes (KB1_0495 and KB1_0553) were, thus, heterologously expressed in *E. coli*, and the purified proteins were experimentally tested for activities with enzymatic assays to confirm or refute the proposed annotations. Further bioinformatics analyses of their sequences suggested their affiliation to potentially new enzyme families within their respective larger enzyme super families.

Results and discussion

Biochemical activities of KB1_0495 and KB1_0553

The heterologously expressed and purified protein from KB1_0495 was tested for the IDH activity using a standard assay (Experimental procedures) to measure the conversion of D-isocitric acid to 2-oxoglutarate and CO_2 using $NADP^+$ or NAD^+ as a cofactor. The pH range and activity of the enzyme (Table 1) were measured using D-isocitric acid as substrate. The enzyme showed IDH activity using both $NADP^+$ and NAD^+ as the cofactor, but the activity with NAD^+ was 65 times lower than with $NADP^+$ (Table 1). This finding confirmed the annotation of KB1_0495 as an $NADP^+$-dependent isocitrate dehydrogenase (*Dm*IDH) proposed by the previous metabolic modelling study (Ahsanul Islam *et al*., 2010). The kinetic parameters for *Dm*IDH were also estimated using both $NADP^+$ and NAD^+ as cofactors (Table 1), and the values obtained for isocitrate and both cofactors are quite

Table 1. Kinetic Parameters of *Dm*IDH and *Dm*PMI from *D. mccartyi*[a]

Enzyme tested (varying substrate)	V_{max} (μmoles·min^{-1}·mg^{-1})	K_m (mM)	k_{cat} (s^{-1})	k_{cat}/K_m ($mM^{-1}·s^{-1}$)
*Dm*IDH (isocitrate)[b]	21.3 ± 2	0.11 ± 0.01	15 ± 1	139.6 ± 1
*Dm*IDH ($NADP^+$)	20.8 ± 2	0.027 ± 0.02	14.6 ± 1	540 ± 1
*Dm*IDH (NAD^+)	0.32 ± 0.05	0.12 ± 0.04	0.22 ± 0.03	2 ± 1
*Dm*PMI (M6P)	1.19 ± 0.2	0.89 ± 0.09	0.84 ± 0.1	0.96 ± 0.3

a. Reaction conditions were as described in Experimental procedures. **b.** Kinetic parameters were determined using $NADP^+$ as cofactor (0.3 mM).

comparable with similar bacterial and archaeal enzymes in the BRENDA database (Chang *et al*., 2009). The higher activity and efficiency of *Dm*IDH with $NADP^+$ are probably linked to its physiological roles in *D. mccartyi*. The incomplete TCA-cycle of these bacteria is mainly used for anabolism (Tang *et al*., 2009; Marco-Urrea *et al*., 2011). Hence, *Dm*IDH plays a crucial role in *D. mccartyi* metabolism by producing the critical biosynthetic precursor 2-oxoglutarate and recycling essential cellular redox currency, NADPH. In fact, most bacteria possess $NADP^+$-dependent IDHs (Chen and Gadal, 1990; Muro-Pastor and Florencio, 1994), and microbes having an incomplete TCA-cycle use IDH to generate precursors (2-oxoglutarate) and reducing power (NADPH) for anabolic biosynthetic pathways (Dean and Golding, 1997; Steen *et al*., 1998). However, NAD^+ may also work as a cofactor for *Dm*IDH *in vivo* because the cellular concentration of NAD^+ is ~ 9 times higher than that of $NADP^+$ in a bacterial cell (Wimpenny and Firth, 1972; Andersen and von Meyenburg, 1977).

The second purified enzyme (KB1_0553) was tested for both PGI/PMI activities using four standard assays (Experimental procedures). Although the PGI activity (Glucose-6-phosphate, G6P ↔ Fructose-6-phosphate, F6P) was tested in both directions with two assays, the enzyme showed no activity with either G6P or F6P as substrates (data not shown). The presence of PMI activity (Mannose-6-phosphate, M6P ↔ Fructose-6-phosphate, F6P) was confirmed in the direction of F6P formation using two assays (Experimental procedures). The pH range and kinetic parameters (Table 1) were also estimated using M6P as substrate. Thus, only the PMI activity was detected and confirmed for KB1_0553 (*Dm*PMI). This activity is typically associated with peptidoglycan and teichoic acid biosynthesis (Kanehisa *et al*., 2011). Therefore, the physiological role of *Dm*PMI in *D. mccartyi* is unclear because they lack a typical bacterial cell wall in favour of an archaeal S-layer like protein and cell membrane (Löffler *et al*., 2012). *Dm*PMI may be involved in cell membrane biogenesis in these bacteria as suggested by the previous transcriptomic study (Ahsanul Islam *et al*., 2014). It can also be involved in the mannosylglycerate (MG) biosynthesis pathway (Fig. 1) because a bifunctional mannosyl-3-phosphoglycerate synthase (EC 2.4.1.217)/phosphatase (EC 3.1.3.70) enzyme encoded by DET1363 (*mgs*D) gene was biochemically characterized from *D. mccartyi* strain 195 (formerly *D. ethenogenes* strain 195) (Empadinhas *et al*., 2004). MG is an unusual compatible solute that helps thermophilic or hyperthermophilic bacteria and archaea to adjust osmotic stress and heat (Santos and da Costa, 2002; Empadinhas and da Costa, 2011). Because *D. mccartyi* strains are halotolerant or slightly halophilic (Empadinhas *et al*., 2004), MG was hypothesized to be involved in cellular osmotic stress adaptation in these bacteria (Hendrickson *et al*., 2002; Empadinhas *et al*., 2004). However, this suggested physiological role is a non-essential or specialized function rather than a major biological function, which probably explains why *Dm*PMI has relatively lower catalytic activity and efficiency (Table 1) than similar enzymes in BRENDA (Chang *et al*., 2009).

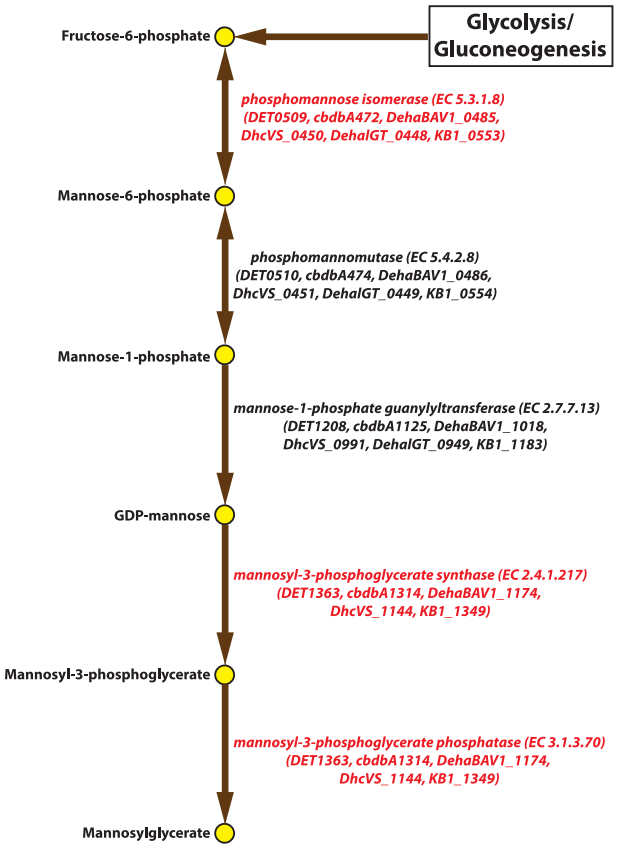

Fig. 1. Mannosylglycerate (MG) biosynthesis pathway in *D. mccartyi*.
Proposed genes and enzymes involved in the compatible solute, MG biosynthesis pathway in *D. mccartyi* are shown. Gene locus names of homologous genes in different *D. mccartyi* genomes encoding the enzymes in each step are shown in parenthesis. Biochemically characterized enzymes are highlighted with the red font colour. Phosphomannose isomerase (EC 5.3.1.8) was characterized in this work (KB1_0553, *Dm*PMI), and the bifunctional mannosyl-3-phosphoglycerate synthase (EC 2.4.1.217)/phosphatase (EC 3.1.3.70) was characterized previously from strain 195 (DET1363, *mgs*D) (Empadinhas *et al*., 2004). The two other genes were identified in *D. mccartyi* genomes during the metabolic modelling study (Ahsanul Islam *et al*., 2010).

Sequence homology and phylogenetic analyses of Dm*IDH and* Dm*PMI sequences*

The sequence homology analysis of *Dm*IDH and *Dm*PMI protein sequences (Fig. 2) revealed the remarkably conserved nature of *Dm*IDH across the domains of life (Fig. 2A) as compared with *Dm*PMI (Fig. 2B). Being a

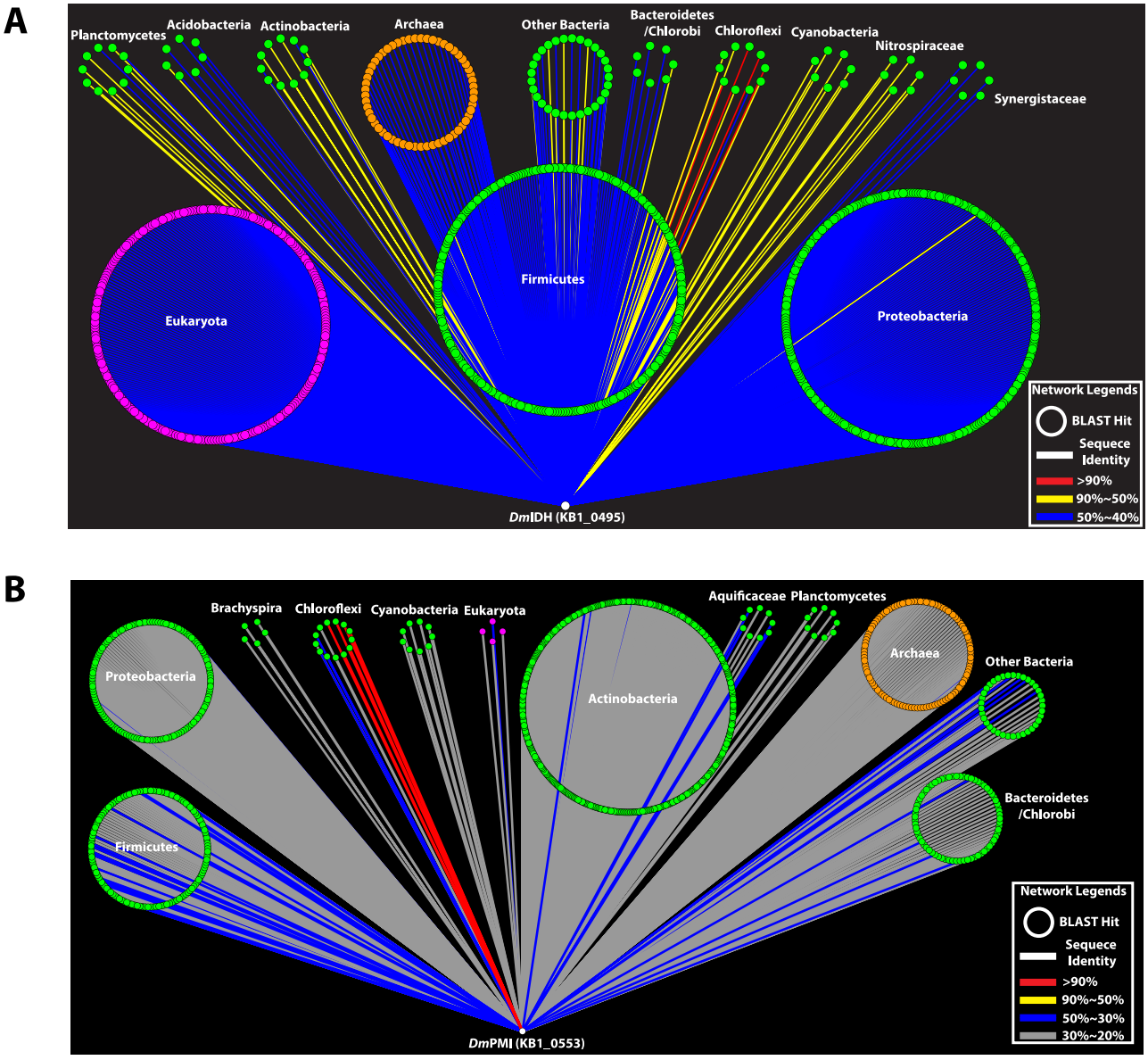

Fig. 2. Sequence homology network of *Dm*IDH and *Dm*PMI.
Homologous protein sequences of *Dm*IDH and *Dm*PMI in archaea, bacteria, and eukarya, identified by blastp in BLAST (Altschul *et al.*, 1997) from UniProt (Apweiler *et al.*, 2012), are shown as nodes, and sequence identities of *Dm*IDH and *Dm*PMI homologs are shown as edges in (A) and (B) respectively. The majority of *Dm*IDH homologs were > 40% identical at the amino acid level (indicated by blue edges), whereas the majority of *Dm*PMI homologs shared < 30% amino acid sequence identity with the *Dm*PMI sequence (indicated by grey edges).

TCA-cycle enzyme, *Dm*IDH was found to share > 40% amino acid sequence identity with other homologous IDHs from eukarya, archaea, and bacteria (Fig. 2A), whereas *Dm*PMI showed < 30% amino acid sequence identity with the majority of its homologs (Fig. 2B). This difference in sequence conservation was also observed from the higher bootstrap values in the *Dm*IDH maximum likelihood (ML) tree (Fig. 3) as compared with those in the ML tree of *Dm*PMI (Fig. 4). The *Dm*IDH tree further showed its separate clustering (Fig. 3) from the previously described (Steen *et al.*, 1997) subfamilies I and II of biochemically characterized IDHs, as well as from subfamily III of NAD^+-dependent eukaryotic IDHs (Steen *et al.*, 1997). Thus, *Dm*IDH belongs to a potentially new subfamily that also includes bacterial IDHs from *Planctomycetes*, *Firmicutes* and *Cyanobacteria* (Fig. 3). Interestingly, no homolog of *Dm*PMI was identified within the three types of PMIs characterized and described previously (Schmidt *et al.*, 1992; Proudfoot *et al.*, 1994). Among the biochemically characterized enzymes, the closest homologs of *Dm*PMI were identified to be archaeal bifunctional PGI/PMIs (Fig. 4), which represent a novel enzyme family

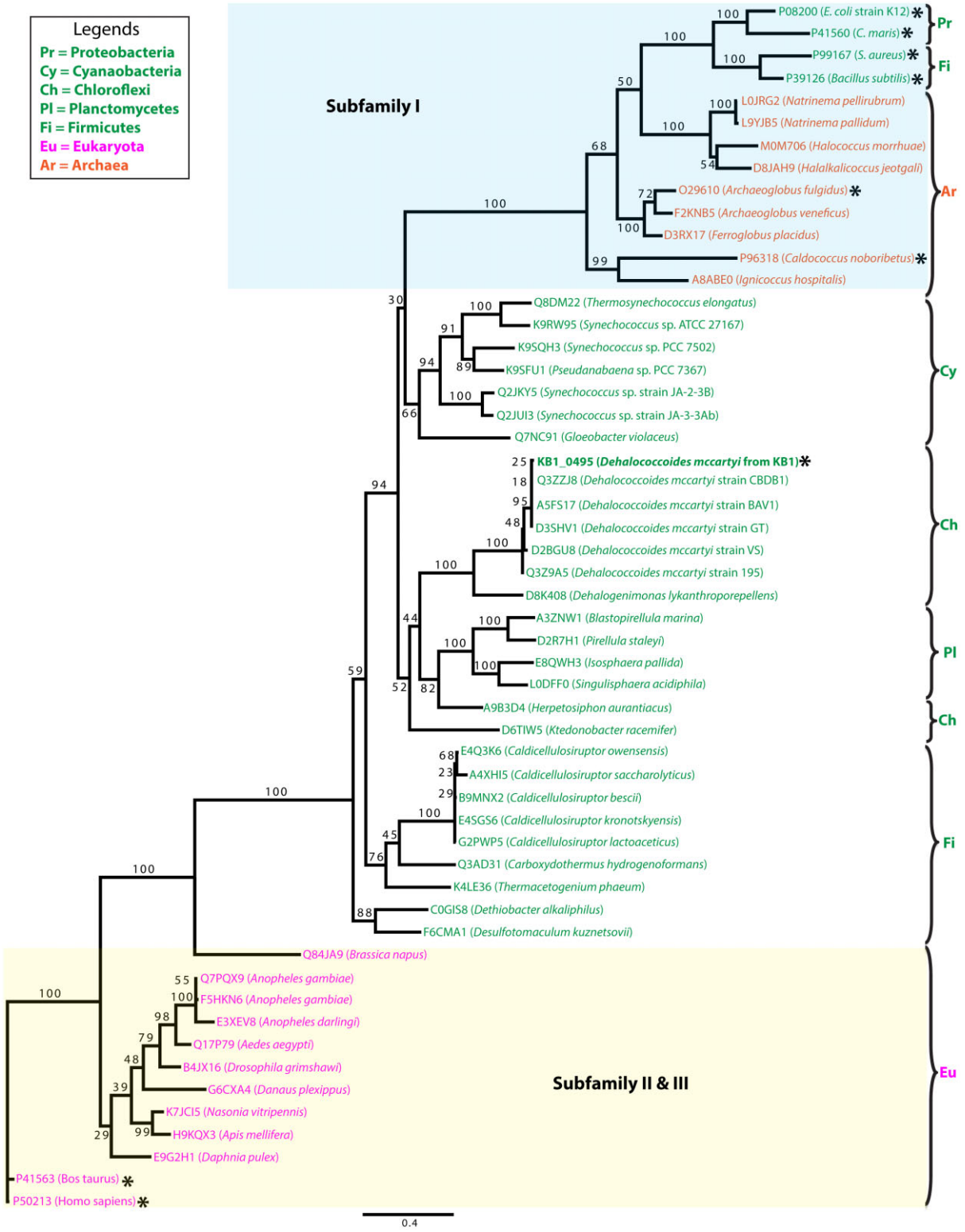

Fig. 3. Phylogenetic analysis of *Dm*IDH protein sequence. Maximum likelihood (ML) tree for *Dm*IDH and its homologous protein sequences was constructed by PHYML (Guindon *et al*., 2010) plugin in GENEIOUS (Biomatters, 2011). Protein sequences were mined from UniProt (Apweiler *et al*., 2012) and aligned with MUSCLE (Edgar, 2004) plugin in GENEIOUS. Then, the ML tree was constructed under WAG (Whelan and Goldman, 2001) model of amino acid substitution with 100 bootstrap resampling trees were conducted. Bootstrap values are shown as branch labels, and the biochemically characterized genes are marked by asterisks. Organism names are coloured according to different kingdoms (Orange = *Archaea*, Green = *Bacteria*, and Purple = *Eukarya*).

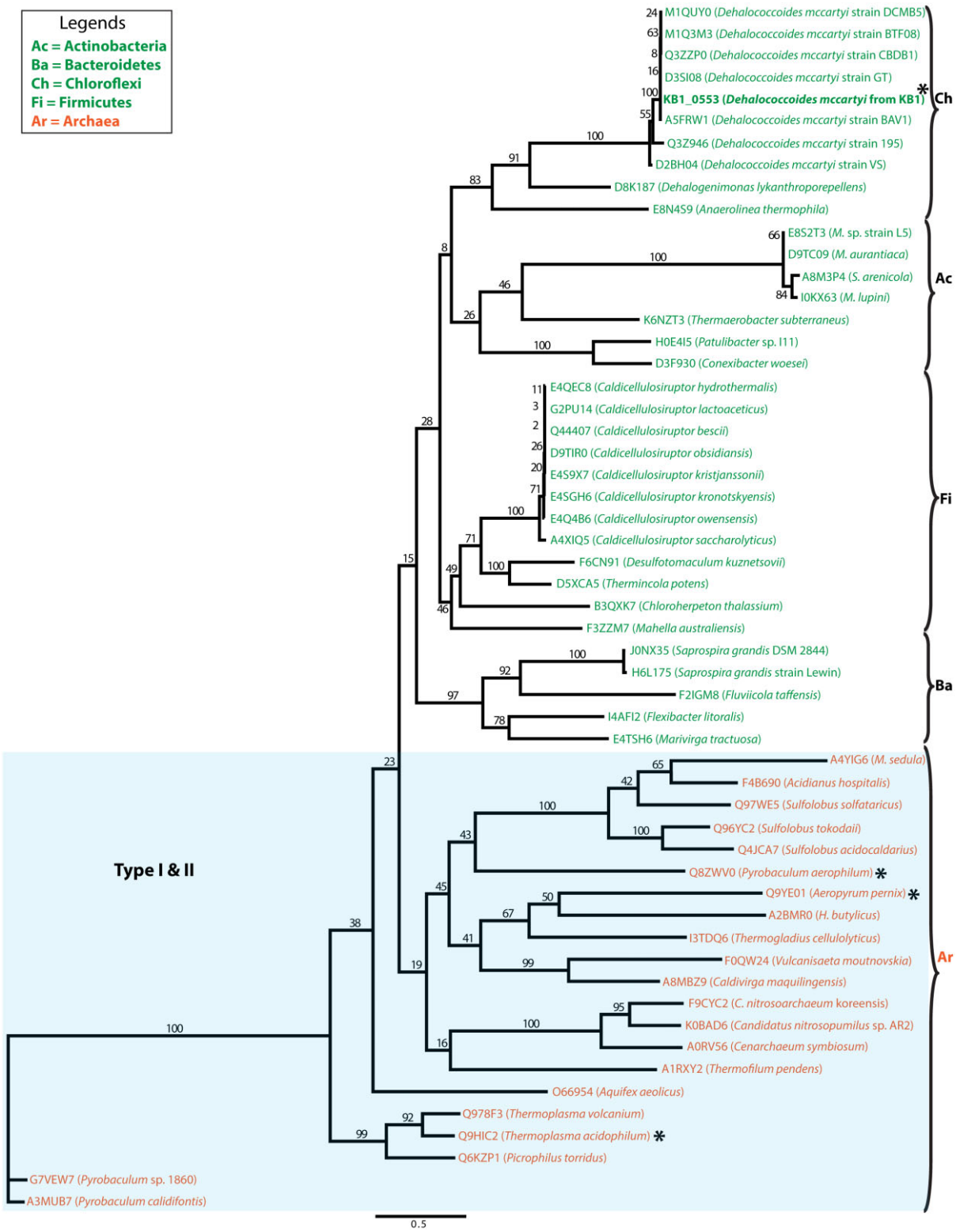

Fig. 4. Phylogenetic analysis of *Dm*PMI protein sequence. Maximum likelihood (ML) tree for *Dm*PMI and its homologous protein sequences was constructed by PHYML (Guindon *et al.*, 2010) plugin in GENEIOUS (Biomatters, 2011). Protein sequences were mined from UniProt (Apweiler *et al.*, 2012) and aligned with MUSCLE (Edgar, 2004) plugin in GENEIOUS. Then, the ML tree was constructed under WAG (Whelan and Goldman, 2001) model of amino acid substitution with 100 bootstrap resampling trees were conducted. Bootstrap values are shown as branch labels, and the biochemically characterized genes are marked by asterisks. Organism names are coloured according to different kingdoms (Orange = *Archaea* and Green = *Bacteria*).

within the PGI superfamily (Hansen *et al*., 2004a,b). Thus, *Dm*PMI likely constitutes a novel class of bacterial PMIs, including the homologs from *Actinobacteria*, *Firmicutes* and *Bacteroidetes* (Fig. 4).

Structure-based analysis of Dm*IDH and* Dm*PMI sequences*

To verify the aforementioned differences of *Dm*IDH and *Dm*PMI from the previously characterized similar enzymes, we conducted further bioinformatics analyses of their sequences. Multiple sequence alignment (MSA) of *Dm*IDH sequence and its biochemically characterized homologs from SWISSPROT identified 66 completely conserved residues (Fig. 5). These included all residues (indicated by blue and red boxes in Fig. 5) involved in substrate and coenzyme binding in *Archaeoglobus fulgidus* and *E. coli* IDHs (Hurley *et al*., 1991; Steen *et al*., 1997; Stokke *et al*., 2007), suggesting a similar reaction mechanism for *Dm*IDH. Although the signature motif of both isocitrate and isopropylmalate dehydrogenases (IDH and IPMDH) was identified in *Dm*IDH (indicated by a green box in Fig. 5), only the IDH activity was tested and confirmed because of its location in an operon containing other putative TCA-cycle genes (Fig. S2). Also, the *D. mccartyi* genomes harbor a putative IPMDH gene (KB1_0839, cbdbA804, DET0826, DhcVS_730, DehaBAV1_0745 and DehalGT_0706) located in the L-leucine biosynthesis operon (Fig. S4). Comparison of the predicted secondary structure of *Dm*IDH (Fig. 5) with the crystal structures of *A. fulgidus* and *E. coli* IDHs (Hurley *et al*., 1991; Stokke *et al*., 2007) showed that most helix and strand regions were conserved among them in spite of the presence of some subtle structural differences. For instance, *Dm*IDH has 12 α-helices and 11 β-strands (Fig. 5), whereas *A. fulgidus* has 18 α-helices, 16 β-strands (Stokke *et al*., 2007) and *E. coli* has 13 α-helices, 12 β-strands (Hurley *et al*., 1991).

MSA of *Dm*PMI sequence with its biochemically characterized or manually reviewed homologs identified only 20 completely conserved residues (Fig. 6). In addition to two signature motifs (marked by blue boxes in Fig. 6) of archaeal PGI/PMIs (Hansen *et al*., 2004b), a SIS (sugar isomerase) domain (marked by a green box in Fig. 6) was identified in *Dm*PMI. All residues proposed to be important for substrate binding and catalysis in archaeal PGI/PMIs (Hansen *et al*., 2004a; Swan *et al*., 2004) are also found to be conserved in *Dm*PMI (marked by red boxes in Fig. 6), except a few notable ones: Thr60, Ser103, Arg152, Ser154, Pro341, and Ile342. The most important change was detected at residue position 154, where a Serine (S) substituted an Arginine (R) found in other archaeal PGI/PMIs (marked by a yellow S in Fig. 6). This residue is pivotal for the catalytic activities of archaeal PGI/PMIs because it stabilizes the formation of crucial enediol intermediates during their PGI activity (Seeholzer, 1993; Hansen *et al*., 2004b; Swan *et al*., 2004). Hence, these changes in the *Dm*PMI sequence are likely responsible for its inability to function as PGI. A similar notion was also obtained from the comparison of the predicted secondary structure of *Dm*PMI (12 α–helices and 9 β-strands) (Fig. 6) with the crystal structure of *Pa*PGI/PMI from *P. aerophilum* (Swan *et al*., 2004). However, the mechanism for PMI activity of *Dm*PMI is likely similar to *Pa*PGI/PMI because the presence of Thr291 in the *Pa*PGI/PMI sequence is key to its PMI activity (Swan *et al*., 2004), and the equivalent residue in *Dm*PMI is an Isoleucine (Ile342) (Fig. 6).

In summary, the two characterized enzymes, *Dm*IDH and *Dm*PMI, from *D. mccartyi* strains in KB-1 likely have reaction mechanisms similar to the previously characterized enzymes although they appear to belong to novel IDH and PMI enzyme families. *Dm*IDH showed a higher catalytic activity with $NADP^+$ as a cofactor than with NAD^+, implicating its involvement in anabolic biosynthetic pathways in *D. mccartyi*, whereas the lower activity of *Dm*PMI suggests that the physiological substrate is possibly a different sugar than M6P, or that it is possibly involved in non-essential physiological roles such as osmotic stress adjustment in these bacteria.

Conclusions

Automated and non-curated primary annotations of genes are necessary but highly problematic if they are wrong. Because initial annotations are often non-specific or incorrect, correcting these annotations is very important and challenging. In this study, corrected or reviewed initial annotations that were proposed from previously published modelling and transcriptomic studies were experimentally tested and shown to be essentially correct, illustrating the utility of metabolic modelling and bioinformatics approaches as important tools of hypothesis generation for gene annotations. Each new biochemical confirmation of gene functions adds to the confidence of propagated annotations, contributing to a stronger database for sequence analysis in general. In the specific case of the unusual organohalide respiring anaerobes *D. mccartyi*, fundamental understanding of the physiology and biochemistry of these organisms will contribute to better deployment of bioremediation approaches for environmental stewardship.

Experimental procedures

Bacterial culture, reagents, and chemicals

Genomic DNA (gDNA) was collected from KB-1, a *D. mccartyi*-containing anaerobic mixed culture growing

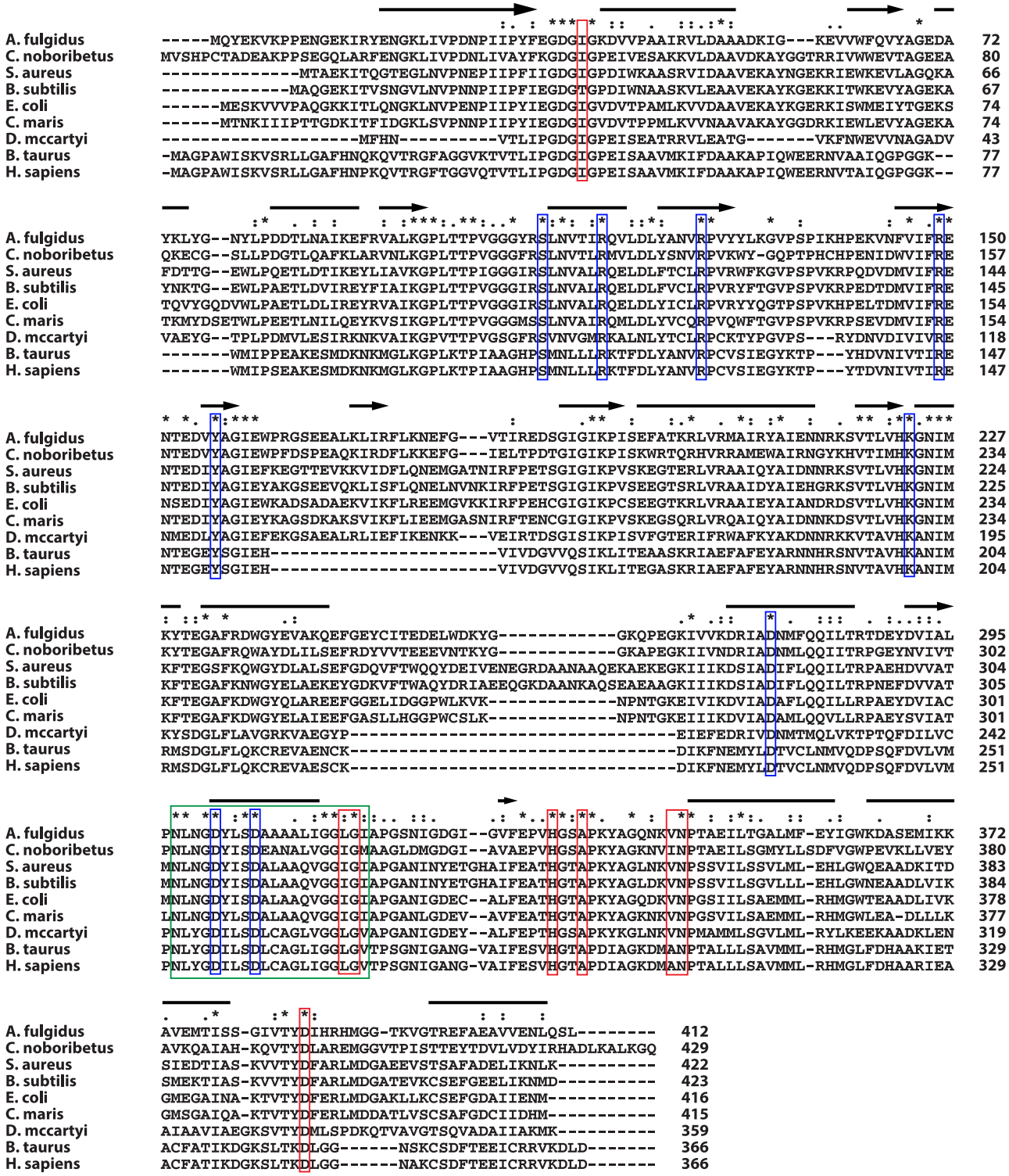

Fig. 5. Structure-based multiple sequence alignment (MSA) of *Dm*IDH.
MSA of *Dm*IDH protein sequence and its homologous, biochemically characterized sequences are shown. Protein sequences were mined from the SWISSPROT curated database (Boeckmann *et al.*, 2003), and MSA was performed by CLUSTALX (Larkin *et al.*, 2007). Completely conserved residues are marked by asterisks, whereas residues reported to be important for substrate and coenzyme binding (Hurley *et al.*, 1991; Stokke *et al.*, 2007) are marked by blue and red boxes respectively. Green box indicates signature motif for isocitrate/isopropylmalate dehydrogenases as identified by SCANPROSITE (de Castro *et al.*, 2006). Protein secondary structure was predicted by PREDICTPROTEIN (Rost and Sander, 1994), and indicated by bars (α-helices) and arrows (β-strands). Protein accession numbers (UniProt) are: *A. fulgidus* (O29610), *C. noboribetus* (P96318), *S. aureus* (P99167), *B. subtilis* (P39126), *E. coli* (P08200), *C. maris* (P41560), *B. taurus* (P41563) and *H. sapiens* (P50213).

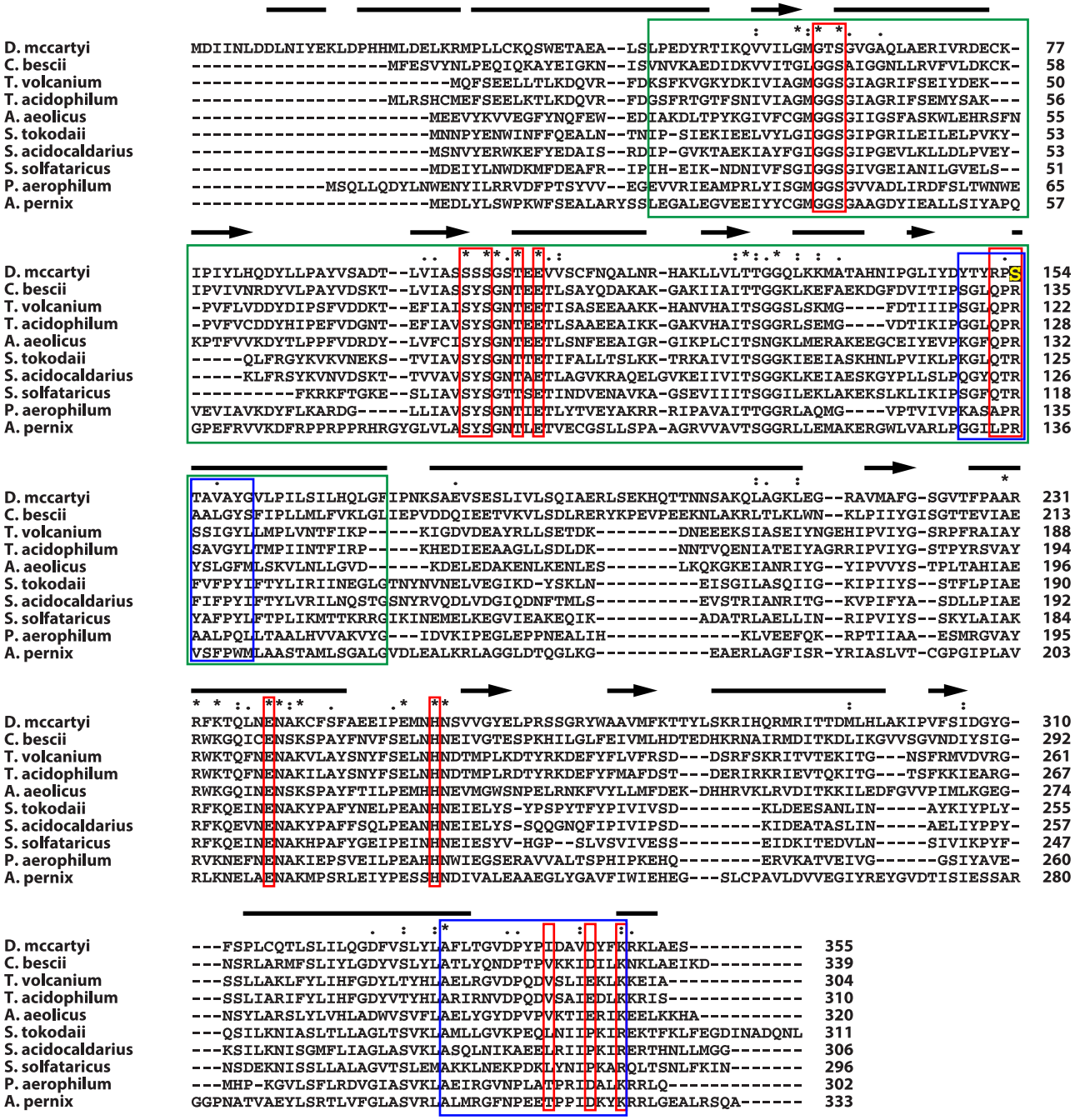

Fig. 6. Structure-based multiple sequence alignment (MSA) of *Dm*PMI.
MSA of *Dm*PMI protein sequence and its homologous, manually reviewed/biochemically characterized sequences are shown. Protein sequences were mined from the SWISSPROT curated database (Boeckmann *et al.*, 2003), and MSA was performed by CLUSTALX (Larkin *et al.*, 2007). Completely conserved residues are marked by asterisks, whereas residues reported to be important for substrate binding and catalysis (Hansen *et al.*, 2004a; Swan *et al.*, 2004) are marked by red boxes. Blue boxes indicate two signature motifs for bifunctional PGI/PMI protein family (Hansen *et al.*, 2004b), and green box indicates Pfam (Punta *et al.*, 2012) SIS (sugar isomerase) domain identified by SCANPROSITE (de Castro *et al.*, 2006). Protein secondary structure was predicted by PREDICTPROTEIN (Rost and Sander, 1994), and indicated by bars (α-helices) and arrows (β-strands). Protein accession numbers (UniProt) are: *C. bescii* (Q44407), *T. volcanium* (Q978F3), *T. acidophilum* (Q9HIC2), *A. aeolicus* (O66954), *S. tokodaii* (Q96YC2), *S. acidocaldarius* (Q4JCA7), *S. solfataricus* (Q97WE5), *P. aerophilum* (Q8ZWV0) and *A. pernix* (Q9YE01).

on TCE and methanol following the procedure described previously (Duhamel and Edwards, 2006). The PCR primers for amplifying *D. mccartyi* gDNA were synthesized by Integrated DNA Technologies (Coralville, IA, USA). Luria broth and terrific broth powder were purchased from EMD Chemicals (Gibbstown, NJ, USA), and the Bradford assay reagent from Bio-Rad (Hercules, CA, USA). Lysozyme, proteinase K, agarose, glycerol, ampicillin, kanamycin, SDS and IPTG were obtained from BioShop (Burlington, ON, Canada), and all other chemicals were purchased from Sigma-Aldrich (St. Louis, MO, USA) with greater than 98% in purity. Nickel-Nitrilotriacetic acid (Ni-NTA) resin and the QIAquick PCR Purification Kit were purchased from Qiagen (Mississauga, ON, Canada), whereas the In-Fusion PCR Cloning Kit was purchased from Clontech (Palo Alto, CA, USA). The commercially available kits were used according to the manufacturers' instructions.

Gene cloning, protein overexpression, and purification

The selected genes (KB1_0495 and KB1_0553) were PCR-amplified using *D. mccartyi* gDNA and the PCR primers containing the restriction sites for BamHI and NdeI, and were cloned into the modified pET-15b vector (Novagen, Madison, WI, USA) containing a 5′ N-terminal hexahistidine tag (6xHis-tag) and an ampicillin resistance gene as described previously (Zhang *et al*., 2001). In the modified vector, the tobacco etch virus protease cleavage site replaced the thrombin cleavage site, and a double stop codon was introduced downstream from the BamHI site (Zhang *et al*., 2001). These vectors were subsequently transformed into *E. coli* strain BL21 (DE3) (Stratagene, La Jolla, CA, USA) for overexpression of the targeted fused genes. The cells were grown aerobically in 1 L flasks containing tryptone-phosphate medium at 37°C and ~ 220 rpm until the OD_{600} reached around 1.0 (approximately in 3 h). Expression of the cloned genes was induced by adding 100 mg IPTG, and cells were harvested the following day by centrifugation (Zhang *et al*., 2001). The overexpressed, fused 6xHis-tagged proteins were purified to more than 95% homogeneity (Fig. S1) using metal-chelate affinity chromatography on nickel affinity resin and gel filtration on a Superdex 200 26/60 column (Amersham Biosciences, Piscataway, NJ, USA) as described before (Zhang *et al*., 2001; Proudfoot *et al*., 2008).

Isocitrate dehydrogenase (IDH) assay

IDH activity in KB1_0495 (*Dm*IDH) was confirmed by an enzymatic assay (Steen *et al*., 1997; 1998) for the reaction described by the following equation:

$$D-isocitric\ acid + NAD(P)^{+} \overset{IDH}{\Leftrightarrow} 2-oxoglutarate + CO_2 + NAD(P)H$$

The standard 1 ml assay contained 50 mM tris-hydrochloride (Tris-HCl) buffer (pH 7.5), 0.3 mM $NADP^+$, 1 mM D-isocitric acid and 10 mM $MgCl_2$. The reaction was started by adding 1 μg of purified protein into the reaction mixture, and the product formation was inferred from the measurement of NAD(P)H formation as indicated by the increase in absorbance at 340 nm and 30°C with a spectrophotometer. The IDH activity in KB1_0495 was also measured using NAD^+ as a cofactor.

Phosphoglucose isomerase (PGI) assay

PGI activity in KB1_0553 (*Dm*PMI) was tested using two standard assays (Hansen *et al*., 2004b) for the reaction described by the following equations:
Assay 1:

$$F6P \overset{PGI}{\Leftrightarrow} G6P$$

$$G6P + NADP^{+} \overset{G6PDH}{\Leftrightarrow} 6PG15L + NADPH$$

where F6P refers to fructose-6-phosphate, G6P refers to glucose-6-phosphate, 6PG15L refers to 6-phospho-D-glucono-1,5-lactone, and G6PDH is glucose-6-phosphate dehydrogenase (EC. 1.1.1.49).
Assay 2:

$$G6P \overset{PGI}{\Leftrightarrow} F6P$$

$$F6P + NADH \overset{M1PDH}{\Leftrightarrow} M1P + NAD^{+}$$

where M1P refers to mannitol-1-phosphate and M1PDH is mannitol-1-phosphate-5-dehydrogenase (EC 1.1.1.17). Reaction mixtures for assay 1 contained 100 mM Tris-HCl (pH 7.5), 0.5 mM $NADP^+$, 10 mM F6P, and 1.1 U of G6PDH (Sigma-Aldrich, St. Louis, MO), and assay 2 contained 100 mM Tris-HCl (pH 7.5), 0.3 mM NADH, 10 mM G6P, and 10 μL of M1PDH. The M1PDH was purified from *E. coli* (Novotny *et al*., 1984) with > 95% purity (see Fig. S1). The reactions were started by adding 1 μg of purified protein into the reaction mixture, and the product formation was inferred from the measurement of NADPH formation in assay 1 and of oxidation of NADH in assay 2 with a spectrophotometer at 340 nm absorbance and 30°C.

Phosphomannose isomerase (PMI) assay

PMI activity in KB1_0553 (*Dm*PMI) was tested with two standard assays (Hansen *et al*., 2004a) for the reactions described by the following equations:

Assay 1:

$$M6P \overset{PMI}{\Leftrightarrow} F6P$$

$$F6P + NADH \overset{M1PDH}{\Leftrightarrow} M1P + NAD^{+}$$

where M6P refers to mannose-6-phosphate.
Assay 2:

$$M6P \overset{PMI}{\Leftrightarrow} F6P$$

$$F6P \overset{PGI}{\Leftrightarrow} G6P$$

$$G6P + NADP^{+} \overset{G6PDH}{\Leftrightarrow} 6PG15L + NADPH$$

The reaction mixture for assay 1 contained 100 mM Tris-HCl (pH 7.5), 0.5 mM NADH, 10 mM M6P, and 10 µl of M1PDH. The M1PDH was purified from *E. coli* (Novotny *et al*., 1984) with > 95% purity (see Fig. S1). In assay 2, the reaction mixture contained 100 mM Tris-HCl (pH 7.5), 0.5 mM $NADP^{+}$, 10 mM M6P and 1.1 U of G6PDH (Sigma-Aldrich, St. Louis, MO) and 1 U of PGI (Sigma-Aldrich, St. Louis, MO). The reactions were started by adding 1 µg of purified protein into the reaction mixture, and the product, F6P formation, was measured by coupling it to the oxidation of NADH in assay 1 and to the formation of NADPH in assay 2. In both instances, the product formation was inferred from the measurement of absorbance with a spectrophotometer at 340 nm and 30°C.

Determination of pH range and kinetic parameters

The pH range of purified KB1_0495 (*Dm*IDH) and KB1_0553 (*Dm*PMI) (Table 1) was determined by measuring their activities at pH values from 6 to 8.5 at 30°C using D-isocitric acid and M6P as substrates, respectively. The enzymatic activity of both purified proteins was also measured at selected pHs with varying concentrations of substrates, D-isocitric acid, M6P and cofactors, $NADP^{+}$ and NAD^{+} at 30°C. These data were, then, fitted to the Michaelis–Menten enzyme kinetics model with the non-linear regression analysis to estimate the maximum enzyme velocity (V_{max}) and the Michaelis constant (K_m) using GraphPad Prism v 5.0 (GraphPad Software, La Jolla, CA, USA). Then, the turnover number (k_{cat}) and the efficiency (k_{cat}/K_m) of both proteins were calculated from V_{max} and K_m data.

Bioinformatics analyses of Dm*IDH and* Dm*PMI sequences*

Homologous protein sequences of *Dm*IDH and *Dm*PMI in eukarya, archaea, and bacteria were identified by blastp in BLAST (Altschul *et al*., 1997) from the UniProt database (Apweiler *et al*., 2012). The sequence homology networks of both *Dm*IDH and *Dm*PMI were constructed and visualized by CYTOSCAPE (Smoot *et al*., 2011) – an open source bioinformatics software platform. The phylogenetic analysis was conducted by the PHYML (Guindon *et al*., 2010) plugin in the GENEIOUS software platform (Biomatters, 2011) to construct the ML trees for both *Dm*IDH and *Dm*PMI sequences and their homologous protein sequences. First, the homologous sequences were mined from UniProt (Apweiler *et al*., 2012) with blastp in BLAST and aligned with the MUSCLE (Edgar, 2004) plugin in GENEIOUS. Then, the ML tree was constructed using the WAG (Whelan and Goldman, 2001) model of amino acid substitution with 100 bootstrap resampling trees were conducted. The multiple sequence alignment of *Dm*IDH and *Dm*PMI protein sequences was performed by CLUSTALX (Larkin *et al*., 2007), and the biochemically characterized homologous protein sequences were mined from the SWISSPROT curated database (Boeckmann *et al*., 2003). The protein secondary structure of *Dm*IDH and *Dm*PMI was predicted by the PREDICTPROTEIN (Rost and Sander, 1994) software.

Conflict of interest

None declared.

References

Adrian, L., Szewzyk, U., Wecke, J., and Görisch, H. (2000) Bacterial dehalorespiration with chlorinated benzenes. *Nature* **408:** 580–583.

Adrian, L., Hansen, S.K., Fung, J.M., Görisch, H., and Zinder, S.H. (2007a) Growth of *Dehalococcoides* strains with chlorophenols as electron acceptors. *Environ Sci Technol* **41:** 2318–2323.

Adrian, L., Rahnenführer, J., Gobom, J., and Hölscher, T. (2007b) Identification of a chlorobenzene reductive dehalogenase in *Dehalococcoides* sp. strain CBDB1. *Appl Environ Microbiol* **73:** 7717–7724.

Ahsanul Islam, M., Edwards, E.A., and Mahadevan, R. (2010) Characterizing the metabolism of *Dehalococcoides* with a constraint-based model. *PLoS Comput Biol* **6:** e1000887. doi:10.1371/journal.pcbi.1000887.

Ahsanul Islam, M., Waller, A.S., Hug, L.A., Provart, N.J., Edwards, E.A., and Mahadevan, R. (2014) New insights into *Dehalococcoides mccartyi* metabolism from a reconstructed metabolic network-based systems-level analysis of *D. mccartyi* transcriptomes. *PLoS ONE* **9:** e94808. doi:10.1371/journal.pone.0094808.

Altschul, S.F., Madden, T.L., Schäffer, A.A., Zhang, J., Zhang, Z., Miller, W., and Lipman, D.J. (1997) Gapped BLAST and PSI-BLAST: a new generation of protein database search programs. *Nucleic Acids Res* **25:** 3389–3402.

Andersen, K.B., and von Meyenburg, K. (1977) Charges of nicotinamide adenine nucleotides and adenylate energy

charge as regulatory parameters of the metabolism in *Escherichia coli*. *J Biol Chem* **252:** 4151–4156.

Apweiler, R., Jesus Martin, M., O'onovan, C., Magrane, M., Alam-Faruque, Y., Antunes, R., *et al*. (2012) Reorganizing the protein space at the Universal Protein Resource (UniProt). *Nucleic Acids Res* **40:** D71–D75.

Biomatters (2011) Geneious v 6.1.5 created by Biomatters. [WWW document]. URL http://www.geneious.com/.

Boeckmann, B., Bairoch, A., Apweiler, R., Blatter, M.-C., Estreicher, A., Gasteiger, E., *et al*. (2003) The SWISS-PROT protein knowledgebase and its supplement TrEMBL in 2003. *Nucleic Acids Res* **31:** 365–370.

de Castro, E., Sigrist, C.J., Gattiker, A., Bulliard, V., Langendijk-Genevaux, P.S., Gasteiger, E., *et al*. (2006) ScanProsite: detection of PROSITE signature matches and ProRule-associated functional and structural residues in proteins. *Nucleic Acids Res* **34:** W362–W365.

Chang, A., Scheer, M., Grote, A., Schomburg, I., and Schomburg, D. (2009) BRENDA, AMENDA and FRENDA the enzyme information system: new content and tools in 2009. *Nucleic Acids Res* **37:** D588–D592.

Chen, R.-D., and Gadal, P. (1990) Structure, functions and regulation of NAD and NADP dependent isocitrate dehydrogenases in higher plants and in other organisms. *Plant Physiol Biochem* **28:** 411–427.

Dean, A.M., and Golding, G. (1997) Protein engineering reveals ancient adaptive replacements in isocitrate dehydrogenase. *Proc Natl Acad Sci USA* **94:** 3104–3109.

Duhamel, M., and Edwards, E.A. (2006) Microbial composition of chlorinated ethene-degrading cultures dominated by *Dehalococcoides*. *FEMS Microbiol Ecol* **58:** 538–549.

Edgar, R.C. (2004) MUSCLE: a multiple sequence alignment method with reduced time and space complexity. *BMC Bioinformatics* **5:** 113.

Empadinhas, N., and da Costa, M.S. (2011) Diversity, biological roles and biosynthetic pathways for sugar-glycerate containing compatible solutes in bacteria and archaea. *Environ Microbiol* **13:** 2056–2077.

Empadinhas, N., Albuquerque, L., Costa, J., Zinder, S., Santos, M., Santos, H., and da Costa, M. (2004) A gene from the mesophilic bacterium *Dehalococcoides ethenogenes* encodes a novel mannosylglycerate synthase. *J Bacteriol* **186:** 4075–4084.

EPA, (2011) *US Environmental Protection Agency* [WWW document]. URL http://www.epa.gov/teach/teachsummaries.html.

Gribble, G.W. (2010) *Naturally Occurring Organohalogen Compounds – A Comprehensive Update*. Vienna, Austria: Springer-Verlag.

Gribble, G.W. (2012) Occurrence of halogenated alkaloids. *Alkaloids Chem Biol* **71:** 1–165.

Guha, N., Loomis, D., Grosse, Y., Lauby-Secretan, B., El Ghissassi, F., Bouvard, V., *et al*. (2012) Carcinogenicity of trichloroethylene, tetrachloroethylene, some other chlorinated solvents, and their metabolites. *Lancet Oncol* **13:** 1192–1193.

Guindon, S., Dufayard, J., Lefort, V., Anisimova, M., Hordijk, W., and Gascuel, O. (2010) New algorithms and methods to estimate maximum-likelihood phylogenies: assessing the performance of PhyML 3.0. *Syst Biol* **59:** 307–321.

Hansen, T., Urbanke, C., and Schönheit, P. (2004a) Bifunctional phosphoglucose/phosphomannose isomerase from the hyperthermophilic archaeon *Pyrobaculum aerophilum*. *Extremophiles* **8:** 507–512.

Hansen, T., Wendorff, D., and Schönheit, P. (2004b) Bifunctional phosphoglucose/phosphomannose isomerases from the archaea *Aeropyrum pernix* and *Thermoplasma acidophilum* constitute a novel enzyme family within the phosphoglucose isomerase superfamily. *J Biol Chem* **279:** 2262–2272.

He, J., Ritalahti, K.M., Yang, K.L., Koenigsberg, S.S., and Löffler, F.E. (2003) Detoxification of vinyl chloride to ethene coupled to growth of an anaerobic bacterium. *Nature* **424:** 62–65.

Hendrickson, E., Payne, J., Young, R., Starr, M., Perry, M., Fahnestock, S., *et al*. (2002) Molecular analysis of *Dehalococcoides* 16S ribosomal DNA from chloroethene-contaminated sites throughout North America and Europe. *Appl Environ Microbiol* **68:** 485–495.

Hug, L., Beiko, R., Rowe, A., Richardson, R., and Edwards, E. (2012) Comparative metagenomics of three *Dehalococcoides*-containing enrichment cultures: the role of the non-dechlorinating community. *BMC Genomics* **13:** 327.

Hug, L.A. (2012) A metagenome-based examination of dechlorinating enrichment cultures: *Dehalococcoides* and the role of the non-dechlorinating microorganisms. In *Cell and Systems Biology*. Toronto, ON, Canada: University of Toronto. http://hdl.handle.net/1807/32742.

Hurley, J.H., Dean, A., Koshland, D.J., and Stroud, R.M. (1991) Catalytic mechanism of NADP(+)-dependent isocitrate dehydrogenase: implications from the structures of magnesium-isocitrate and NADP+ complexes. *Biochemistry* **30:** 8671–8678.

Jayachandran, G., Gorisch, H., and Adrian, L. (2004) Studies on hydrogenase activity and chlorobenzene respiration in *Dehalococcoides* sp. strain CBDB1. *Arch Microbiol* **182:** 498–504.

Johnson, D.R., Brodie, E.L., Hubbard, A.E., Andersen, G.L., Zinder, S.H., and Alvarez-Cohen, L. (2008) Temporal transcriptomic microarray analysis of *Dehalococcoides ethenogenes* strain 195 during the transition into stationary phase. *Appl Environ Microbiol* **74:** 2864–2872.

Johnson, D.R., Nemir, A., Andersen, G.L., Zinder, S.H., and Alvarez-Cohen, L. (2009) Transcriptomic microarray analysis of corrinoid responsive genes in *Dehalococcoides ethenogenes* strain 195. *FEMS Microbiol Lett* **294:** 198–206.

Kanehisa, M., Goto, S., Sato, Y., Furumichi, M., and Tanabe, M. (2011) KEGG for integration and interpretation of large-scale molecular data sets. *Nucleic Acids Res* **40:** D109–114. [Epub: Nov 10].

Krajmalnik-Brown, R., Hölscher, T., Thomson, I.N., Saunders, F.M., Ritalahti, K.M., and Löffler, F.E. (2004) Genetic identification of a putative vinyl chloride reductase in *Dehalococcoides* sp. strain BAV1. *Appl Environ Microbiol* **70:** 6347–6351.

Kube, M., Beck, A., Zinder, S.H., Kuhl, H., Reinhardt, R., and Adrian, L. (2005) Genome sequence of the chlorinated compound-respiring bacterium *Dehalococcoides* species strain CBDB1. *Nat Biotechnol* **23:** 1269–1273.

Larkin, M.A., Blackshields, G., Brown, N., Chenna, R., McGettigan, P., McWilliam, H., *et al*. (2007) Clustal W and Clustal X version 2.0. *Bioinformatics* **23:** 2947–2948.

Lee, P.K., Dill, B., Louie, T., Shah, M., Verberkmoes, N., Andersen, G., *et al*. (2012) Global transcriptomic and proteomic responses of *Dehalococcoides ethenogenes* strain 195 to fixed nitrogen limitation. *Appl Environ Microbiol* **78:** 1424–1436.

Löffler, F.E., Yan, J., Ritalahti, K.M., Adrian, L., Edwards, E.A., Konstantinidis, K.T., *et al*. (2012) *Dehalococcoides mccartyi* gen. nov., sp. nov., obligate organohalide-respiring anaerobic bacteria, relevant to halogen cycling and bioremediation, belong to a novel bacterial class, *Dehalococcoidetes classis* nov., within the phylum *Chloroflexi*. *Int J Syst Evol Microbiol* **63:** 625–635. [ePub Apr 27].

Madigan, M.T., Martinko, J.M., and Parker, J. (2010) *Brock Biology of Microorganisms*, 13th edn. San Francisco, CA, USA: Benjamin Cummings.

Magnuson, J.K., Stern, R.V., Gossett, J.M., Zinder, S.H., and Burris, D.R. (1998) Reductive dechlorination of tetrachloroethene to ethene by a two-component enzyme pathway. *Appl Environ Microbiol* **64:** 1270–1275.

Magnuson, J.K., Romine, M.F., Burris, D.R., and Kingsley, M.T. (2000) Trichloroethene reductive dehalogenase from *Dehalococcoides ethenogenes*: sequence of tceA and substrate range characterization. *Appl Environ Microbiol* **66:** 5141–5147.

Marco-Urrea, E., Paul, S., Khodaverdi, V., Seifert, J., von Bergen, M., Kretzschmar, U., and Adrian, L. (2011) Identification and characterization of a Re-citrate synthase in *Dehalococcoides* strain CBDB1. *J Bacteriol* **193:** 5171–5178.

Markowitz, V.M., Chen, I., Palaniappan, K., Chu, K., Szeto, E., Grechkin, Y., *et al*. (2012) IMG: The Integrated Microbial Genomes database and comparative analysis system. *Nucleic Acids Res* **40:** D115–D122.

Maymó-Gatell, X., Chien, Y., Gossett, J.M., and Zinder, S.H. (1997) Isolation of a bacterium that reductively dechlorinates tetrachloroethene to ethene. *Science* **276:** 1568–1571.

Morris, R.M., Sowell, S., Barofsky, D., Zinder, S., and Richardson, R. (2006) Transcription and mass-spectroscopic proteomic studies of electron transport oxidoreductases in *Dehalococcoides ethenogenes*. *Environ Microbiol* **8:** 1499–1509.

Morris, R.M., Fung, J.M., Rahm, B.G., Zhang, S., Freedman, D.L., Zinder, S., and Richardson, R.E. (2007) Comparative proteomics of *Dehalococcoides* spp. reveals strain-specific peptides associated with activity. *Appl Environ Microbiol* **73:** 320–326.

Muro-Pastor, M.I., and Florencio, F.J. (1994) NADP(+)-isocitrate dehydrogenase from the cyanobacterium *Anabaena* sp. strain PCC 7120: purification and characterization of the enzyme and cloning, sequencing, and disruption of the icd gene. *J Bacteriol* **176:** 2718–2726.

Müller, J.A., Rosner, B.M., von Abendroth, G., Meshulam-Simon, G., McCarty, P.L., and Spormann, A.M. (2004) Molecular identification of the catabolic vinyl chloride reductase from *Dehalococcoides* sp. strain VS and its environmental distribution. *Appl Environ Microbiol* **70:** 4880–4888.

Nelson, D.L., and Cox, M.M. (2006) *Lehninger Principles of Biochemistry*. New York, NY, USA: W. H. Freeman and Company.

Nijenhuis, I., and Zinder, S.H. (2005) Characterization of hydrogenase and reductive dehalogenase activities of *Dehalococcoides ethenogenes* strain 195. *Appl Environ Microbiol* **71:** 1664–1667.

Novotny, M.J., Reizer, J., Esch, F., and Saier, M.J. (1984) Purification and properties of D-mannitol-1-phosphate dehydrogenase and D-glucitol-6-phosphate dehydrogenase from *Escherichia coli*. *J Bacteriol* **159:** 986–990.

Proudfoot, A.E., Turcatti, G., Wells, T.N., Payton, M.A., and Smith, D.J. (1994) Purification, cDNA cloning and heterologous expression of human phosphomannose isomerase. *Eur J Biochem* **219:** 415–423.

Proudfoot, M., Sanders, S.A., Singer, A., Zhang, R., Brown, G., Binkowski, A., *et al*. (2008) Biochemical and structural characterization of a novel family of cystathionine beta-synthase domain proteins fused to a Zn ribbon-like domain. *J Mol Biol* **375:** 301–315.

Punta, M., Coggill, P.C., Eberhardt, R.Y., Mistry, J., Tate, J., Boursnell, C., *et al*. (2012) The Pfam protein families database. *Nucleic Acids Res* **40:** D290–D301.

Quevillon, E., Silventoinen, V., Pillai, S., Harte, N., Mulder, N., Apweiler, R., and Lopez, R. (2005) InterProScan: protein domains identifier. *Nucleic Acids Res* **33:** W116–W120.

Rajesh, T., Song, E., Kim, J., Lee, B., Kim, E., Park, S., *et al*. (2012) Inactivation of phosphomannose isomerase gene abolishes sporulation and antibiotic production in *Streptomyces coelicolor*. *Appl Microbiol Biotechnol* **93:** 1685–1693.

Rost, B., and Sander, C. (1994) Combining evolutionary information and neural networks to predict protein secondary structure. *Proteins* **19:** 55–72.

Santos, H., and da Costa, M. (2002) Compatible solutes of organisms that live in hot saline environments. *Environ Microbiol* **4:** 501–509.

Schmidt, M., Arnold, W., Niemann, A., Kleickmann, A., and Pühler, A. (1992) The *Rhizobium meliloti pmi* gene encodes a new type of phosphomannose isomerase. *Gene* **122:** 35–43.

Seeholzer, S.H. (1993) Phosphoglucose isomerase: A ketol isomerase with aldol C2-epimerase activity. *Proc Natl Acad Sci USA* **90:** 1237–1241.

Seshadri, R., Adrian, L., Fouts, D.E., Eisen, J.A., Phillippy, A.M., Methe, B.A., *et al*. (2005) Genome sequence of the PCE-dechlorinating bacterium *Dehalococcoides ethenogenes*. *Science* **307:** 105–108.

Smoot, M.E., Ono, K., Ruscheinski, J., Wang, P.L., and Ideker, T. (2011) Cytoscape 2.8: new features for data integration and network visualization. *Bioinformatics (Oxf)* **27:** 431–432.

Steen, I.H., Lien, T., and Birkeland, N. (1997) Biochemical and phylogenetic characterization of isocitrate dehydrogenase from a hyperthermophilic archaeon, *Archaeoglobus fulgidus*. *Arch Microbiol* **168:** 412–420.

Steen, I.H., Madsen, M., Birkeland, N.-K., and Lien, T. (1998) Purification and characterization of a monomeric isocitrate dehydrogenase from the sulfate-reducing bacterium *Desulfobacter vibrioformis* and demonstration of the

presence of a monomeric enzyme in other bacteria. *FEMS Microbiol Lett* **160:** 75–79.
Stokke, R., Karlström, M., Yang, N., Leiros, I., Ladenstein, R., Birkeland, N., and Steen, I. (2007) Thermal stability of isocitrate dehydrogenase from *Archaeoglobus fulgidus* studied by crystal structure analysis and engineering of chimers. *Extremophiles* **11:** 481–493.
Swan, M.K., Hansen, T., Schönheit, P., and Davies, C. (2004) A novel phosphoglucose isomerase (PGI)/phosphomannose isomerase from the crenarchaeon *Pyrobaculum aerophilum* is a member of the PGI superfamily: structural evidence at 1.16-A resolution. *J Biol Chem* **279:** 39838–39845.
Tang, S., Chan, W., Fletcher, K., Seifert, J., Liang, X., Löffler, F., *et al.* (2013) Functional characterization of reductive dehalogenases by using blue native polyacrylamide gel electrophoresis. *Appl Environ Microbiol* **79:** 974–981.
Tang, Y.J., Yi, S., Zhuang, W.Q., Zinder, S.H., Keasling, J.D., and Alvarez-Cohen, L. (2009) Investigation of carbon metabolism in *Dehalococcoides ethenogenes* strain 195 by use of isotopomer and transcriptomic analyses. *J Bacteriol* **191:** 5224–5231.
Wang, S., Chng, K.R., Wilm, A., Zhao, S., Yang, K.-L., Nagarajan, N., and He, J. (2014) Genomic characterization of three unique *Dehalococcoide*s that respire on persistent polychlorinated biphenyls. *PNAS* **111:** 12103–12108.
Whelan, S., and Goldman, N. (2001) A general empirical model of protein evolution derived from multiple protein families using a maximum-likelihood approach. *Mol Biol Evol* **18:** 691–699.
Wimpenny, J.W.T., and Firth, A. (1972) Levels of nicotinamide adenine dinucleotide and reduced nicotinamide adenine dinucleotide in facultative bacteria and the effect of oxygen. *J Bacteriol* **111:** 24–32.
Zhang, R.G., Skarina, T., Katz, J., Beasley, S., Khachatryan, A., Vyas, S., *et al.* (2001) Structure of *Thermotoga maritima* stationary phase survival protein SurE: a novel acid phosphatase. *Structure* **9:** 1095–1106.

Supporting information

Additional Supporting Information may be found in the online version of this article at the publisher's web-site:

Fig. S1. SDS-PAGE of (A) *Dm*IDH, (B) *Dm*PMI, and (C) M1PDH.
Fig. S2. Orthologous gene neighborhood analysis of isocitrate dehydrogenase (IDH) from *D. mccartyi*.
Fig. S3. Orthologous gene neighborhood analysis of hypothetical protein/SIS domain protein from *D. mccartyi*.
Fig. S4. Orthologous gene neighborhood analysis of 3-isopropylmalate dehydrogenase (IPMDH) from *D. mccartyi*